Top Quark Threshold Production at a $\gamma\gamma$ Collider at Next-to-Next-to-Leading Order

Andrzej Czarnecki
Department of Physics, University of Alberta
Edmonton, AB   T6G 2J1, Canada
E-mail: czar@phys.ualberta.ca

Kirill Melnikov
Stanford Linear Accelerator Center
Stanford University, Stanford, CA 94309
E-mail: melnikov@slac.stanford.edu

The next-to-next-to-leading order (NNLO) QCD corrections to top quark threshold pair production in $\gamma\gamma$ collisions are computed. The NNLO effects turn out to be significant. Threshold cross sections in $\gamma\gamma$ and e^+e^- collisions are compared.

PACS numbers: 13.60.Hb, 12.38.Bx, 14.65.Ha

arXiv:hep-ph/0108233 v1   28 Aug 2001

Studies of threshold production of top quark pairs will provide information about Standard Model parameters and a window to "New Physics" phenomena. Because the t quark decays fast compared to the strong interaction time scale, even the threshold top pair production in e^+e^- or $\gamma\gamma$ collisions can be described using perturbative QCD [1]. However, close to the threshold, the cross section is enhanced by the strong attraction between the quark and the antiquark and an all-order resummation of the Coulomb effects is required. The magnitude of the threshold cross section and the position of its peak are sensitive to the top quark mass and width, as well as the strong coupling constant α_s, and can help determine those parameters with high precision [2, 3]. In addition, precision measurements in the threshold region at the Next Linear Collider (NLC) will probe electroweak interactions of the t quarks and be sensitive to "New Physics".

A particularly interesting environment for studying "New Physics" effects in the top production is the $\gamma\gamma$ collider mode of the NLC, with laser beams backscattered from the high-energy e^+ and e^- as the source of the colliding photons [4]. It has been pointed out [5, 6] that the process $\gamma\gamma \to t\bar{t}$ is twice as sensitive to anomalous photon-top quark couplings as $e^+e^- \to t\bar{t}$, and in addition is free from contamination by the $Zt\bar{t}$ coupling. It will therefore allow searches for anomalous couplings of the top quark to photons, in particular the electric dipole moment. Although precision studies might be feasible only at the NLC, the observation of $\gamma\gamma \to t\bar{t}$ may be possible already at the LHC [7].

Although the threshold production cross section can be computed perturbatively, it is not clear how well the series converges. Recently, the renormalization group technique was employed [8] to sum up large logarithmic corrections appearing in threshold problems. It was applied

to $\sigma(e^+e^- \to t\bar{t})$ at the threshold in [9] and an achievement of a 3% accuracy in the normalization of the cross section was claimed. However, it is conceivable that possible large non-leading-logarithmic effects may spoil this picture. To a large extent, study of the $t\bar{t}$ threshold production cross section in the $\gamma\gamma$ mode might help in an assessment of the situation and provide an additional test of the assumptions of the resummation program.

In general, behavior of the $t\bar{t}$ threshold cross sections is rather similar in e^+e^- and $\gamma\gamma$ collisions; the difference comes from the fact that the quarks are mainly produced in spin one and spin zero state in e^+e^- and $\gamma\gamma$ collisions, respectively. Since the Coulomb interaction does not depend on the spin, this fact does not affect the behavior of the leading order cross section but, since relativistic corrections do depend on the total spin of the produced fermion pair, it becomes important in higher orders.

There is yet another interesting feature of the top quark threshold production in $\gamma\gamma$ collisions [4]. In contrast to an e^+e^- collider, manipulating polarization of the incoming photons can suppress the S-wave production and provide a possibility to study the P-wave threshold production without the huge S-wave background. All these features of the top quark threshold in $\gamma\gamma$ collisions make it a very interesting laboratory for studying the non-relativistic QCD dynamics of a heavy quark antiquark system, determining the standard model parameters, and searching for "New Physics".

A known problem with this program is the monochromaticity of the photon beams at the NLC where a typical energy spread is currently estimated to be about 10% of the total energy (see e.g. [10]). This may hamper the threshold studies since a large energy spread will wash out any pronounced signal at the top threshold. It remains to be seen if this difficulty can be overcome.

Much effort has already been spent on theoretical studies of $\sigma(\gamma\gamma \to t\bar{t})$ with polarized photons. Away from the threshold, one-loop QCD corrections were computed in [11]. Close to the threshold, the cross section $\sigma(e^+e^- \to t\bar{t})$ has been studied in NLO in [4]. Recently, studies of NNLO corrections to $\sigma(e^+e^- \to t\bar{t})$ were completed and the appropriate effective field theory framework for studying higher order corrections to the threshold phenomena was formulated (see [3] and references therein). Applying similar techniques to $\gamma\gamma \to t\bar{t}$, it is in principle straightforward to obtain the NNLO corrections to this process; the major obstacle has been the lack of the two-loop matching coefficient for an effective operator responsible for the leading order transition $\gamma\gamma \to t\bar{t}$ at the threshold. In this paper we describe the calculation of this matching coefficient and present the NNLO corrections to $\sigma(\gamma\gamma \to t\bar{t})$ at the threshold.

Close to the threshold, the produced top quarks are non-relativistic so that it is reasonable to expand the production amplitudes in powers of the relative velocity β of t and $\bar{t}$. The Born amplitude for $\gamma\gamma \to t\bar{t}$ with $\mathcal{O}(\beta^2)$ accuracy can be written as

$$\mathcal{M} = -8i\pi\alpha Q_t^2 \phi^+ \left[\mathcal{M}_S + \mathcal{M}_P\right]\chi, \qquad (1)$$

where $Q_t = 2/3$ is the electric charge of the top quark, ϕ and χ are the top and anti-top spinors. The amplitudes that give rise to the production of the $t\bar{t}$ state in S and P waves are, respectively

$$\mathcal{M}_S = \left(1 + \frac{(\vec{p}\vec{n})^2}{m^2} - \frac{\vec{p}^2}{2m^2}\right)i\vec{n}\cdot[\vec{e}_1 \times \vec{e}_2], \qquad (2)$$

$$\mathcal{M}_P = \frac{(\vec{p}\vec{n})(\vec{\sigma}\vec{n})(\vec{e}_1\vec{e}_2) + (\vec{p}\vec{e}_1)(\vec{\sigma}\vec{e}_2) + (\vec{p}\vec{e}_2)(\vec{\sigma}\vec{e}_1)}{m}.$$

In these formulas, $\vec{n}$ is a unit vector along the photon flight direction, $\vec{p}$ is the top quark three-momentum and $\vec{e}_{1,2}$ are the polarization vectors of the colliding photons. From now on we will consider the incoming photons to be circularly polarized. If the two photons have opposite polarizations, the S wave production amplitude vanishes. As a consequence, only $\mathcal{M}_P$ contributes to the top production and the cross section at the threshold behaves as $\sigma_{+-} \sim \beta^3$. If the photon helicities are the same, the top quarks are mainly produced in the S wave with a small admixture of the P wave appearing in the NNLO.

It is customary to define a normalized unpolarized cross section, $R_{\gamma\gamma} = \sigma(\gamma\gamma \to t\bar{t})/\sigma_0$, with $\sigma_0 = 4\pi\alpha^2/(3s)$, and decompose it into contributions with the same and opposite photon helicities, $R_{\gamma\gamma} = (R^{++} + R^{+-})/2$, where we have used $R^{++} = R^{--}$ and $R^{+-} = R^{-+}$, valid for electromagnetic processes. Let us consider the case of the two photons with equal helicities and select the contribution of the S wave. (The case of the P wave production has been investigated earlier in the literature (for the most recent discussion see [12]) and, because of its relative $\mathcal{O}(\beta^2)$ suppression, we do not have much to add to this issue.) In case of the S wave,

the quarks are produced in a spin singlet state. The expression for the cross section in the regime $\alpha_s \ll \beta \ll 1$ reads:

$$R_S^{++} = 6Q_t^4 N_c\beta\left(1 - \frac{\beta^2}{3}\right)$$

$$\cdot\left[1 + C_F\left(\frac{\alpha_s}{\pi}\right)\Delta^{(1)} + C_F\left(\frac{\alpha_s}{\pi}\right)^2\Delta^{(2)}\right], \quad (3)$$

where $\beta = \sqrt{1 - 4m^2/s}$. Also,

$$\Delta^{(1)} = \frac{\pi^2}{2\beta} - \left(5 - \frac{\pi^2}{4}\right) + \frac{\pi^2}{2}\beta + \mathcal{O}\left(\beta^2\right). \qquad (4)$$

The two-loop corrections can be decomposed into four parts, arising from the abelian and non-abelian gluon effects, and to light quark and top quark vacuum polarization insertions in the one-loop correction. Neglecting terms of $\mathcal{O}(\beta)$, the two-loop corrections are

$$\Delta^{(2)} = C_F\Delta_A + C_A\Delta_{NA} + T_R N_L\Delta_L + T_R N_H\Delta_H, \quad (5)$$

$$\Delta_A = \frac{\pi^4}{12\beta^2} + \left(-\frac{5}{2} + \frac{1}{8}\pi^2\right)\frac{\pi^2}{\beta}$$

$$+ \frac{27}{8}\pi^2 + \frac{25}{4} + \frac{35}{192}\pi^4 - 2\pi^2\ln(2\beta) + 2x_A;$$

$$\Delta_{NA} = \left(\frac{31}{72} - \frac{11}{12}\ln(2\beta)\right)\frac{\pi^2}{\beta}$$

$$+ \pi^2\left(\frac{5}{4} - \ln(2\beta)\right) + 2x_{NA};$$

$$\Delta_L = \left(-\frac{5}{18} + \frac{1}{3}\ln(2\beta)\right)\frac{\pi^2}{\beta} + 2x_L;$$

$$\Delta_H = 2x_H. \qquad (6)$$

In the above formulas the terms x_A, x_{NA}, x_L, x_H are related to the hard renormalization of the operator $\phi^+\vec{n}\cdot[\vec{e}_1 \times \vec{e}_2]\chi$ responsible for $\gamma\gamma \to t\bar{t}$ transition at the threshold:

$$x_A = -21.02; \quad x_{NA} = -4.79;$$
$$x_L = -0.565; \quad x_H = 0.224. \qquad (7)$$

To evaluate the hard renormalization factors we have used some of the results obtained for the para-positronium decay [13, 14]. In addition, to find x_{NA} which is our main new result here, we had to evaluate the non-abelian diagrams (see Fig. 1(a-e)) and massless insertions in the one-loop diagrams (an example is shown in Fig. 1(f)). Here we briefly summarize those calculations. Diagram 1(a) is the simplest two-loop non-abelian contribution. It is both ultraviolet (UV) and infrared (IR) finite and we evaluate it using Monte Carlo integration over six Feynman parameters. (We use FORM [15] for symbolic manipulations and Vegas [16] for numerical integrations.) Diagram 1(b) is UV divergent. To compute it we use a trick: assign mass M to the quark line (inside the loops) and expand the diagram in the ratio $t = m^2/M^2$, treating M as much larger than m.
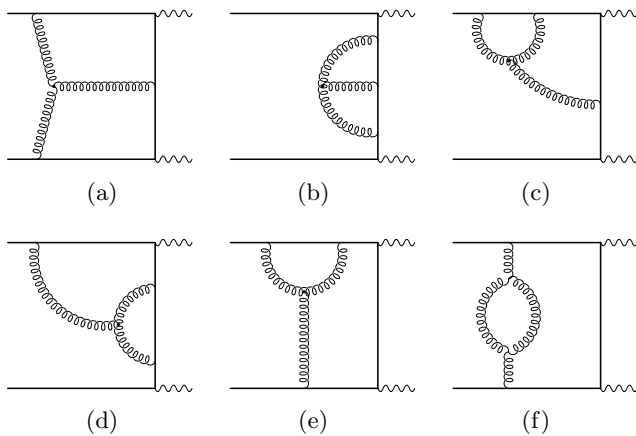
FIG. 1: Examples of non-abelian hard corrections to $\gamma\gamma \to t\bar{t}$ computed in this paper. In addition, we include diagrams similar to (f) with gluon, Faddeev-Popov ghost and fermion loops inserted in all one-loop corrections.

At the end we have to evaluate the sum of the resulting series at $t = 1$. It is sufficient to compute only a few first terms of the series in t if we change the variables, $t \to -4w/(1 + w)^2$, expand in w, and evaluate the new series at $w = 2\sqrt{2} - 3 \simeq -0.17$.

Diagrams (c) and (d) are also UV-divergent, with a subdivergence in the non-abelian vertex correction and an overall divergence. It is useful to first remove the subdivergence by subtracting a product of one-loop diagrams which can be evaluated analytically. Next, the remaining overall divergence is removed by subtracting a similar two-loop amplitude which depends either only on the external quark momentum (for (c)) or only on the spatial photon momentum (for (d)). The resulting finite integrals are evaluated with Vegas, while the subtracted divergent pieces can be computed either exactly (for (c)) or with the expansion used for the diagram (b).

The only IR-divergent non-trivial two-loop diagram is (e). It also contains a UV-subdivergence which we remove in the same way as in (c) and (d). The IR-divergence is subtracted by neglecting the loop momentum in the "t-channel" quark propagator. That subtraction can be computed analytically, since it is simply a 2-loop vertex diagram at threshold, of the type for which we developed a general algorithm in an earlier study [17]. The finite difference is evaluated with Vegas.

We did not include effects of the $\gamma\gamma \to gg$ scattering via light quark boxes. We have checked with a rough approximation that this finite and gauge-invariant subset contributes only insignificantly.

Using the result (3) it is easy to obtain the top threshold production cross section for the photons with equal helicities close to the threshold. In doing that, we follow the approach described in Ref. [18]. Let us first present a general formula for the resummed cross section for two different choices of the photon helicities. We find:

$$R_S^{++} = \frac{24\pi N_c Q_t^4}{m_t^2} C_h$$
$$\times \mathrm{Im}\left\{\left(1 - \frac{5}{6}\beta^2\right) G^{\mathrm{sing}}(0, 0, E + i\Gamma_t)\right\}, \quad (8)$$

where C_h is the hard renormalization factor and G^{sing} is the Green's function of the spin singlet state of the $t\bar{t}$ pair including relativistic corrections and corrections to the Coulomb potential (see [18] for details).

As we already mentioned, there is also a P wave contribution to the ++ cross section at NNLO. It is suppressed by $\mathcal{O}(\beta^2)$ relative to the S wave and working to NNLO we need to know it only to leading order. Since for the photon helicities +− the top pair is also produced in the P wave, there is a leading-order relation between R_P^{++} and R^{+-},

$$R^{+-} = \frac{4}{3} R_P^{++}, \quad (9)$$
$$R^{+-} = \frac{32\pi Q_t^4 N_c}{m_t^4} \partial_{\mathbf{x}} \partial_{\mathbf{y}} \mathrm{Im}\, G(\mathbf{x}, \mathbf{y}, E + i\Gamma_t)|_{\mathbf{x}=\mathbf{0}, \mathbf{y}=\mathbf{0}}.$$

Numerically (see e.g. [12]) the P wave contribution is small; the corresponding values of R^{+-} are $\sim 5 \times 10^{-2}$. For this reason, we do not consider the P wave contribution in what follows. In Fig. 2 we present the LO, NLO and NNLO excitation curves for R_S^{++} computed using the pole mass of the top quark. As is clearly seen from this plot, the NNLO corrections to the normalization of the cross section are quite large: close to the peak they are about $20 - 30\%$. The position of the peak of the cross section from which the mass of the top quark is to be determined suffers from significant shifts when one goes from LO to NNLO. All these features are quite similar to the known behavior of $e^+e^- \to t\bar{t}$ at the threshold [3].

Let us now address these problems in turn. It was argued [19, 20] in connection with the threshold production of $t\bar{t}$ in e^+e^- collisions that significant shifts in the position of the peak are the consequences of the fact that the pole mass scheme is unstable against radiative corrections. The way out of this problem is to adopt a different mass definition which will have such a stability. In Fig. 3 we show the S-wave part of the cross section, parameterized by the so-called kinetic mass [21]. We observe that the stability of the peak does improve significantly, a behavior familiar from $e^+e^- \to t\bar{t}$ studies.

Let us now discuss the corrections to the peak height. Again, the situation is similar to $e^+e^- \to t\bar{t}$ but the corrections are larger. Since the height of the cross section is controlled by the wave function at the origin, $\psi(0)$, of the $t\bar{t}$ ground state, it is easy to understand what is happening by looking at the $\ln\alpha_s$ enhanced corrections to $\psi(0)$ computed in [22]. Neglecting effects of the running of the coupling constant, they read

$$\psi^2(0) = \psi_0^2(0)\left[1 - \alpha_s^2 \ln\alpha_s (7.55 - 1.19\, S(S+1))\right.$$
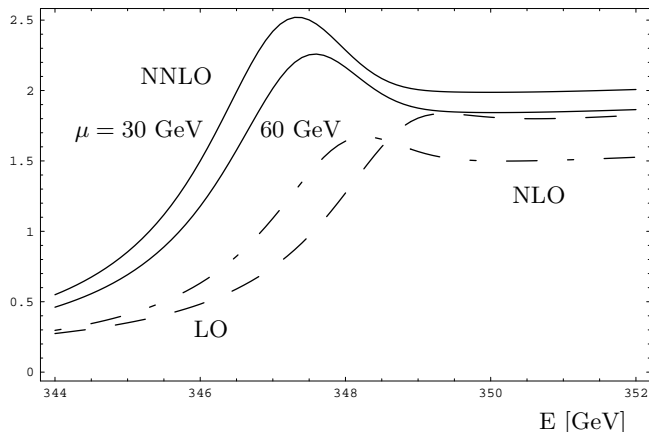$$\left. + \alpha_s^3 \ln^2\alpha_s (-9.48 + 0.99\, S(S+1))\right]. \quad (10)$$

FIG. 2: R_S^{++} at LO, NLO and NNLO. Top quark pole mass $m_t = 175.05$ GeV width $\Gamma_t = 1.43$ GeV are used. The hard renormalization scale and the factorization scale are equal to the top quark mass ($\alpha_s(m_t) = 0.109$). The soft renormalization scale is 60 GeV ($\alpha_s(60$ GeV$) = 0.127$) but we also show the NNLO curve for the soft renormalization scale 30 GeV to demonstrate large changes with the coupling constant scale variation.
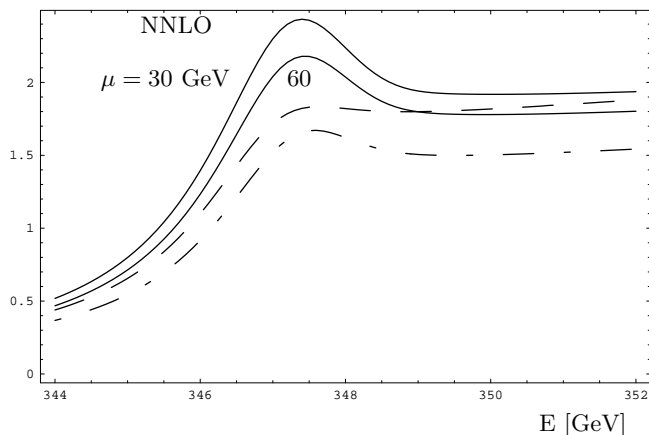

FIG. 3: R_S^{++} parameterized with the kinetic mass $m_{\rm kin}(15$ GeV$) = 173.10$ GeV. Other parameters are the same as in Fig. 2. Dashed, dashed-dotted and solid curves are LO, NLO and NNLO approximations, respectively.

The $\mathcal{O}(\alpha_s^3)$ (N^{3}LO) leading logarithmic effects are included in this formula. From Eq. (10) one sees that there is, effectively, a compensation between spin-dependent and spin-independent terms in the correction to the wave function at the origin; since the top quarks are produced in the spin-singlet state in $\gamma\gamma \to t\bar{t}$, the corrections in this case are expected to be larger than in $e^+e^- \to t\bar{t}$. Note also that in both cases the $\alpha_s^3 \ln \alpha_s$ corrections are negative, so that the NNLO curves shown in Fig. 2 are expected to be pushed down in N^{3}LO, which clearly illustrates the sign-alternating nature of the perturbative series. The success of the resummation program [9] for $e^+e^- \to t\bar{t}$ is related to this property of the series; for this reason one can expect a significant improvement in the
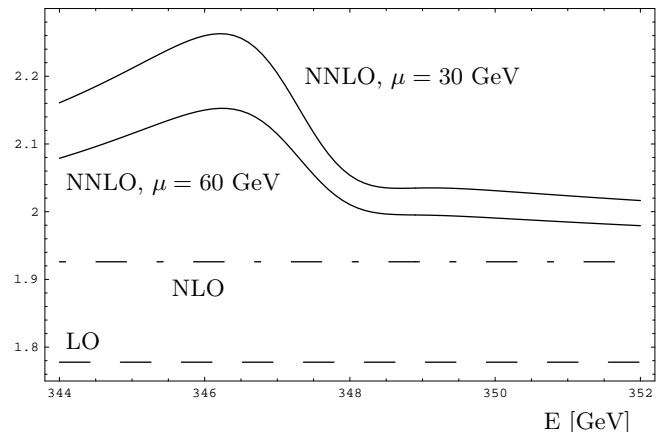

FIG. 4: The ratio of R_S^{++} and R_e in the threshold region at LO, NLO and NNLO (with two different soft renormalization scales) parameterized by kinetic mass $m_{\rm kin}(15$ GeV$)$.

stability of the height of the cross section also in $\gamma\gamma \to t\bar{t}$ once the resummation program is carried out.

It is also interesting to consider the ratio of the top threshold production cross sections in e^+e^- and $\gamma\gamma$ collisions, plotted in Fig. 4. We see that the ratio is energy independent at LO and NLO, since in these orders the spin of the $t\bar{t}$ pair decouples. However, at the NNLO the non-relativistic Hamiltonian depends on the spin of the $t\bar{t}$ pair and the ratio of the cross-sections becomes energy dependent. This results in large corrections to the ratio in the vicinity of the peak. Away from the peak where the bound state dynamics is not very important and the ratio is, essentially, given by the hard renormalization factors of the production currents, the convergence of the perturbative series for the ratio is quite good.

The NNLO corrections to the top pair threshold production in $\gamma\gamma$ collisions, which we have completed by evaluating the non-abelian hard renormalization factor, turn out to be large. This is similar to the process $e^+e^- \to t\bar{t}$. In both cases we see that the position of the cross section peak is stabilized when a short-distance quark mass definition is used, but the height of the peak is changed significantly by the NNLO corrections. We have argued that the structure of the NNLO corrections to $\gamma\gamma \to t\bar{t}$ at the threshold is rather similar to that of $e^+e^- \to t\bar{t}$; in particular the normalization of the cross section is determined by sign-alternating series. This suggests that if the renormalization group improvement, applied to $e^+e^- \to t\bar{t}$ in [9] is applied to $\gamma\gamma \to t\bar{t}$, one can expect significant improvement in the stability of the normalization of the production cross section. For this reason, in the future, it would be interesting to resum the logarithmic corrections $\mathcal{O}(\ln(\beta))$ for $\gamma\gamma \to t\bar{t}$, along the lines of such an analysis for the e^+e^- annihilation [9]. We hope that a combined analysis of both processes will shed new light on the behavior of higher-order corrections to the threshold processes and allow to reach better theoretical precision.

[1] V. S. Fadin and V. A. Khoze, JETP Lett. **46**, 525 (1987), [Pisma ZhETF **46** 417 (1987)]; Sov. J. Nucl. Phys. **48**, 309 (1988), [Yad. Fiz. **48**, 487 (1988)].

[2] E. Accomando *et al.*, Phys. Rept. **299**, 1 (1998).

[3] A. H. Hoang *et al.*, Eur. Phys. J. direct **C3**, 1 (2000).

[4] I. I. Bigi, F. Gabbiani, and V. A. Khoze, Nucl. Phys. **B406**, 3 (1993).

[5] J. L. Hewett, Int. J. Mod. Phys. **A13**, 2389 (1998).

[6] E. Boos *et al.*, hep-ph/0103090.

[7] K. Piotrzkowski, Phys. Rev. **D63**, 071502 (2001).

[8] M. E. Luke, A. V. Manohar, and I. Z. Rothstein, Phys. Rev. **D61**, 074025 (2000).

[9] A. H. Hoang, A. V. Manohar, I. W. Stewart and T. Teubner, Phys. Rev. Lett. **86**, 1951 (2001) and hep-ph/0107144.

[10] T. Abe *et al.*, Resource Book for Snowmass 2001, hep-ex/0106058.

[11] B. Kamal, Z. Merebashvili, and A. P. Contogouris, Phys. Rev. **D51**, 4808 (1995).

[12] A. A. Penin and A. A. Pivovarov, Nucl. Phys. **B550**, 375 (1999).

[13] A. Czarnecki, K. Melnikov, and A. Yelkhovsky, Phys. Rev. Lett. **83**, 1135 (1999), E: ibid. **85**, 2221 (2000).

[14] A. Czarnecki, K. Melnikov, and A. Yelkhovsky, Phys. Rev. A **61**, 052502 (2000), E: ibid. **62**, 059902 (2000).

[15] J. A. M. Vermaseren, math-ph/0010025.

[16] G. P. Lepage, J. Comp. Phys. **27**, 192 (1978), and Cornell preprint CLNS-80/447.

[17] A. Czarnecki and K. Melnikov, Phys. Rev. Lett. **80**, 2531 (1998).

[18] K. Melnikov and A. Yelkhovsky, Nucl. Phys. **B528**, 59 (1998).

[19] M. Beneke, Phys. Lett. **B434**, 115 (1998).

[20] A. H. Hoang, M. C. Smith, T. Stelzer, and S. Willenbrock, Phys. Rev. **D59**, 114014 (1999).

[21] I. Bigi, M. Shifman, N. Uraltsev, and A. Vainshtein, Phys. Rev. **D56**, 4017 (1997).

[22] B. A. Kniehl and A. A. Penin, Nucl. Phys. **B577**, 197 (2000).